ULTRASONIC INVESTIGATION OF n-Si SAMPLES

P. Petculescu[*], J. Matei

Department of Physics, the Ovidius University of Constanta, 8700, Romania

The paper aims to cast a new light on the accuracy of ultrasound based measurement of elastic parameters for crystalline materials. We have measured the values of elastic parameters and their temperature variation for n-Si sample. We present two sets of empirical relations vs. the adiabatic approximation and the thermal coefficient of elastic constants. Our results are in agreement with the modern theory of crystal lattices elaborated by Leibfriend and Ludwig, which gives a general relationship between the elastic constants and the temperature considering the anharmonic nature of the atomic oscillations. Knowing the temperature variation of nonlinearity parameter, we estimated the degradation of the material. The results of our measurements of the elastic constants demonstrate that, in the investigated temperature range, the anisotropy factor is a constant and is equal to 1.54 ± 0.06.

1. Introduction

Ultrasonic is a nondestructive method for the evaluation of the microstructure and associated mechanical parameters. Microstructural characterization of the material which includes the determination of dislocations, grain size material anisotropy, cracks, inclusions and geometry, plays an important role in ensuring the quality of the estimation of mechanical properties and the determination of the amount and the rate of the degradation of structures and components [1]. Ultrasonic velocity techniques enable us to determine the elastic [2] and inelastic parameters of the materials including elastic module, the nonlinearity parameter and the anisotropy factor without harming the materials being tested.

2. Experimental

2.1. Theory

2.1.1 *Elastic constants and the adiabatic approximation*

By pulse-echo method the elastic constants of a solid can be determined. To this aim it is necessary to experimentally measure the longitudinal and transversal sound velocities in the sample. The sample subjected to the experiments that is Si semiconductor, bears three elastic constants corresponding to the cubical system. Crystallographically, the cubic system employs the following relations for the outcome of the first conversion, namely the elastic constants C_{ij} [3]:

$$C_{11} = \rho v_L^2 [100]; \; C_{44} = \rho v_T^2 [100]; \; C_{11} + C_{12} + C_{44} = 3\rho v_L^2 [111] \tag{1}$$

where ρ – is the sample density.

[*] Corresponding author: petculescu@univ-ovidius.ro

One can easily notice the fact that C_{11} and C_{44} can be obtained in a more direct manner from velocity data, were C_{12} can be obtained only indirectly. In order to measure the elastic constants using the above – stated relations, the propagation direction is considered parallel to the required crystallographic axis and the ultrasound waves are plane waves [4].

Given the fact that the actual experimental conditions do not generally follow these requirements there are errors between the transducer and the examined sample, due to the following causes:

- the misalignment between the crystal orientation and the required crystallographic axis;
- the diffraction which appear because the transducer has a finite diameter and the acoustic pressure received in different points do not have the same phase;
- the fact that in the near field (Fresnel zone), the presence of the lateral surfaces limiting the propagation medium influences the oscillation mode and the propagation velocity becomes dependent on the lateral size of the sample and the wavelength.

In the adiabatic approximation we assumed zero change in the thermal energy during the successive contraction-dilatation processes which occurs while ultrasonic waves propagate through the material. In ambient temperature conditions, the elastic constants are influenced by the energy of the atomic oscillations, which are assumed to have the following temperature dependence [5]

$$C_{ij}(T) = C_{ij}^{0}(A - BT) \tag{2}$$

where C_{ij}^{0} corresponds to 0 K.

Making allowances for the fact that the dilatation process and the temperature variation of the elastic constants are included by the anharmonic nature of atomic oscillations, a more general model can be applied:

$$C_{ij}(T) = C_{ij}^{0}[1 - D_{ij}E(T)] \tag{3}$$

where D_{ij} – are the anharmonic coefficients. According to [6], the appearance of higher order terms in the series expansion for the mean energy $E(T)$, leads to a curvature in the high-temperature range of the elastic constants vs. temperature. Experimentally the graph has been shown to exhibit a linear portion in this temperature range, which enables us to disconsider the higher order terms of the series [6]. Thus $E(T) = K_{B}T$, where K_{B} is the Boltzmann constant, will be a reasonable linear approximation for the energy of the atomic oscillation, allowing the temperature dependence of the elastic constants to be expressed as:

$$C_{ij}(T) = C_{ij}^{0}(1 - D_{ij}k_{B}T) \tag{4}$$

2.1.2   *The thermal coefficient of the elastic constant*

The velocity of a longitudinal wave propagating along the [100] axis of the cubic system is given by the equation (1)

$$v_{L[100]} = (C_{11}/\rho)^{1/2} \tag{5}$$

where C_{11} – is an elastic constant and ρ is the material density. Differentiating the equation (5) with respect to temperature, one obtains:

$$\frac{dv_{L}}{dT} = \frac{1}{2\rho}\left(\frac{C_{11}}{\rho}\right)^{-\frac{1}{2}}\left(\frac{dC_{11}}{dT} - \frac{C_{11}}{\rho}\cdot\frac{d\rho}{dT}\right) \tag{6}$$

Because $\rho \approx \rho_{0}(1 - 3\alpha\Delta T)$, where ρ_{0} is the density at temperature T_{0} and α is the thermal coefficient of linear expansion, on can write:

$$\frac{d\rho}{dT} = -3\alpha\rho_{0}. \tag{7}$$

Hence the ecuation (6) can be written as:

$$\frac{2}{v_L} \cdot \frac{dv_L}{dT} \approx \frac{1}{C_{11}} \cdot \frac{dC_{11}}{dT} + 3\alpha \qquad (8)$$

Because $\dfrac{dv}{v} = \dfrac{\Delta v}{v}$ $\dfrac{2}{v_L} \cdot \dfrac{dv_L}{dT} = \dfrac{2}{v_L} \cdot \dfrac{\Delta v_L}{\Delta T}$ one obtains:

$$\frac{1}{C_{11}} \cdot \frac{\Delta C_{11}}{\Delta T} \approx \frac{2}{v_L} \frac{\Delta v_L}{\Delta T} - 3\alpha \qquad (9)$$

where $\dfrac{2}{v_L} \dfrac{\Delta v_L}{\Delta T}$ is the velocity temperature coefficient and $\dfrac{1}{C_{11}} \cdot \dfrac{\Delta C_{11}}{\Delta T}$ is the thermal coefficient of the corresponding elastic constant. Identically, for the transversal ultrasonic velocity v_T for [100] axis, one can write:

$$\frac{1}{C_{44}} \cdot \frac{\Delta C_{44}}{\Delta T} \approx \frac{2}{v_T} \frac{\Delta v_T}{\Delta T} - 3\alpha \qquad (10)$$

with $\Delta T = T - T_0$. In this approximation:

$$C_{ij}(T) = C_{ij}^0(T)\left(1 - \frac{1}{C_{ij}} \cdot \frac{\Delta C_{ij}}{\Delta T} \cdot \Delta T\right). \qquad (11)$$

2.1.3   Nonlinearity parameter

The ultrasonic wave propagating through a solid can produce a waveform distortion induced by the micro structural properties of the solid. This waveform distortion is characterized by the existence of a second harmonic whose amplitude is proportional to the square of the amplitude of the fundamental and to the nonlinearity parameter β. The degree of material degradation can be evaluated by measuring the nonlinearity parameter of the ultrasonic wave propagating through the material [7]. In this work we want to estimate the temperature effect on the nonlinearity parameter for all directions. The nonlinearity parameter has the form [8]:

$$\beta = -\left(3 + \frac{K_3}{K_2}\right) \qquad (12)$$

where K_2 – is a linear combination of the second elastic constants and K_3 – is a linear combination of the third-order elastic constants [9]. According to the crystallographic axis, K_2 and K_3 are given as it follows:

$$
\begin{aligned}
&K_{2[100]} = C_{11};\ K_{2[100]} = \tfrac{1}{2}(C_{11} + C_{22} + 2C_{44});\ K_{2[111]} = 1/3(C_{11} + 2C_{12} + 4C_{44})\\
&K_{1[100]} = C_{111};\ K_{3[110]} = \tfrac{1}{4}(C_{111} + 3C_{112} + 12C_{166})\\
&K_{3[111]} = 1/9(C_{111} + 6C_{112} + 12C_{144} + 24C_{166} + 2C_{123} + 16C_{456})
\end{aligned}
\qquad (13)
$$

and the nonlinearity parameter:

$$
\begin{aligned}
&\beta_{[100]} = -(3 + K_{3[100]}/K_{2[100]});\ \beta_{[110]} = -(3 + K_{3[110]}/K_{2[110]})\\
&\beta_{[111]} = -(3 + K_{3[111]}/K_{2[111]})
\end{aligned}
\qquad (14)
$$

2.1.4   Thermoelastic modulus

It is known that excessive thermal gradients induce stresses that may initiate dislocation generation during the growth of semiconducting materials. The thermal stress calculations entail the elastic constants of the single crystal in the form of a factor designated as thermoelastic modulus M. For the cubic system the thermoelastic modulus can be expressed in terms of the elastic constants [10],[11]:

$$M = \alpha \cdot \frac{6C_{44}(c_{11} + 2C_{12})}{C_{11} + 2C_{12} + 4C_{44}} \tag{15}$$

where α is the thermal coefficient of the linear expansion.

2.1.5   Bulk modulus

The other parameter is the compressibility modulus B which has the form [12]:

$$B = 1/3 \ (C_{11} + 2C_{12}) \tag{16}$$

All these parameters mentioned above, which can characterize the material microstructure, depend on the elastic constants C_{ij}. That is why it is important to determine these constants and their dependence on temperature.

2.2. Modeling

The fixed-mark interferometer pulse-echo method was employed for an experimental determination of [100] and [111] ultrasonic velocities, at f = 4 MHz center frequency launched by a 20 mm diameter transducer. The ultrasonic equipment consisted of an ultrasonic instrument SONIC 136 Ultra (Staveley Instrument Corporation) The fixed-mark interferometer method [13] representing an improvement of the classical interferometer method has been used in order to determine experimentally the propagation velocities. This new method consists of the following steps:
-    make the first pulse-echo to appear on the oscilloscope scale;
-    displace (shift) the reflector pointer until the liquid overlaps with the one through the sample;
-    read the position on the gradation ruler and on the micrometric quadrate marking it by "x";
-    slowly operate the horizontal switch to bring the two overlapped echoes at position 0 on the oscilloscope scale (this position is considered to be brought in front of the upwards flank of the pulse-echo);
-    shift the reflector pointer until the echo through the liquid reaches position 10 on the oscilloscope scale, mark the distance read on the ruler by 'n'.

Thus, the oscilloscope scale has been fitted i.e. ten positions on the scale correspond to n-millimeters on the quadrate ruler of the reflector pointer. Then we have the echo going through the liquid at the position 0, where it overlaps with the one through the sample. The fitting has been performed at the room temperature by increasing the temperature of the sample. Thus we get a displacement to the right of the sample echo, e.g. the sample echo reaches position 2 on the oscilloscope screen, for temperature T_1. In this case, the distance spanned through the water is D = x + 2n/10. For another temperature T_2, the pulse-echo is at position 3.5 and D = x + 3.5n/10. Marking "n_p" the pulse-echo position and "l" the pulse length, we get the general expression D = x + n_pn/10 and the propagation velocity of the ultrasonic waves through the sample at temperature T is:

$$v(t) = v_w(20°C)[1/x + n_p n/10] \tag{17}$$

If by heating at a higher temperature the echo through the sample overtakes the one through the liquid corresponding to position 10, the range scale of the device is changed. Probing at high temperatures was made possible using an Al buffer-rod interposed between the transducer and the sample. We conceived a practical solution for the transducer-buffer-sample (TBS) system in order to overcome the difficulties arising from the fluctuation and non-uniformity of the acoustic pressure across and along the sample in high temperature conditions as well as to maintain and accurately measure a constant temperature along the sample. The oven was provided with an internal ceramic cylinder with the diameter equal to that of the sample. One end of the buffer is inserted into the cylinder which is in contact with the sample, the other end (approx. 65% of its length) being fitted to the ultrasonic transducer. To avoid excessive heating of the transducer, the external end of the buffer is submitted to an uniform air-draft (Fig. 1a).
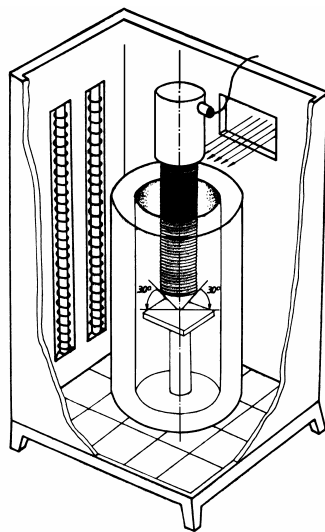
Fig. 1a. The oven with the ceramic cylinder
and the transducer-buffer-sample
(TBS) system.
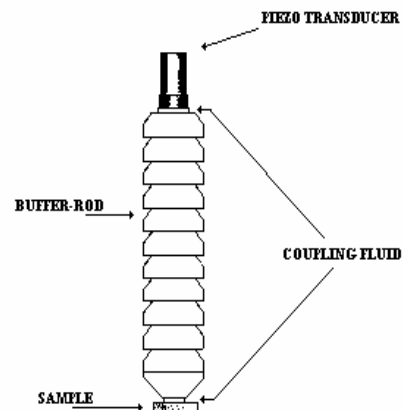
Fig. 1b. Transducer – buffer-rod
– sample system.

The Al buffer-rod has low acoustic attenuation; eleven grooves were performed all over its lateral surface in order to minimize acoustic losses due to lateral reflections. The ultrasonic energy concentration on the sample is enhanced through the 30°-cut truncated cones profile on the sampling end (Fig. 1b). A chromium-aluminium thermocouple is inserted at the center of the examined sample in an orifice practiced in the ceramic filter shielding the sample. The inside diameter of the ceramic filter fits the sample diameter. T 4203 silicone paste was employed to provide the acoustic coupling of the buffer with the sample. On the fixed-mark interferometer based on the determination of ultrasound propagation velocities, water exhibits a 2.5 m/s velocity variation per C°. Therefore, velocity stability requirement was imposed. That problem was solved by replacing water with a mixture of water (80%) and ethanol (20%).

The ultrasonic velocity data and the conversion outcomes were plotted against temperature, employing three methods: (experimental method); method T_1 – empirical method using adiabatic approximation (4) and method T_2 – empirical method using the thermal coefficient of elastic constants (relation 11). The elastic constants were determined in the temperature range 273 K – 900 K.

3. Results on n-Si sample

The n-Si sample has the following parameters: ρ=2330 Kg/m^3, $a_{[111]}$ = 13 mm, $a_{[100]}$ = 13 mm with diameter ϕ = 11.5 mm and N = 6.8 10^{15} cm^{-3} and resistivity = 0.52 Ω cm. Using the adiabatic

approximation (method T_1) we obtained the following empirical relations for the elastic constants of semiconductor Si and this results were corroborated the theoretical relation issued by Simon [6]:

$$C_{11}(TK) = 172.6 \ (1 - 70.3 \times 10^{-6}T)$$
$$C_{12}(TK) = 66.2 \ (1 - 94.4 \times 10^{-6}T) \qquad (18)$$
$$C_{44}(TK) = 82.4 \ (1 - \ 80 \times 10^{-6}T)$$

Table 1.

Authors	0 K				273 K			
	[16]	[17]	[18]	we	[19]	[16]	[17]	we
C_{11}	166	167.5	165	172	167.4	165.7	165.6	167.7
C_{44}	80.1	80.3	79	82.4	79.6	79.6	79.5	80.7
C_{12}	64.2	64.8	64.5	66.2	65.2	63.9	63.9	65.2

C_{ij}^0 values for the 0 K and 273 K, compared to other authors.

We determined from the slope of the ultrasound velocity as a function of temperature, the velocity temperature coefficient $1/v \ \Delta v/\Delta T$ and knowing the thermal coefficient of linear expansion α for the Si sample, we find the thermal coefficient of elastic constant $1/C_{ij} \ \Delta C_{ij}/\Delta T$. So, by applying equation (11) where $C_{ij}^0 (T)$ are elastic constants values at 273 K, we can give empirical method T_2:

$$C_{11}(TK) = 167.7 \ (1 - 64 \times 10^{-6} \ \Delta T)$$
$$C_{44}(TK) = 80.7 \ (1 - 58.4 \times 10^{-6} \Delta T) \qquad (19)$$

where $\Delta T = T - 273$ K.

We can conclude that for the Si sample we can draw three plots against temperature for the elastic constants: the experimental, the adiabatic approximation (method T_1) and the thermal coefficient of the elastic constants (method T_2). Using method T_2 we can determine only C_{11} and C_{44}, which are directly derived from v_L and v_T. To prove that the values, which were found for C_{ij} at 0K through extrapolation and those for 273 K, are valid, we give in Table 1 the results obtained by of other authors. Fig. 2 a,b,c for Si, shows the plots of elastic constants C_{ij} against temperature made by these three methods, above mentioned.
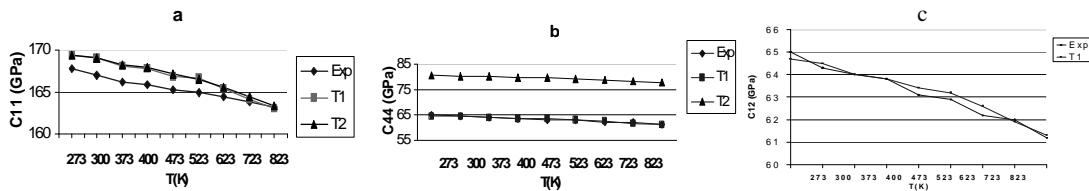
Fig. 2. Temperature plots of the elastic constants for each of the three methods.

The analysis of the plot shows that the curves drawn from experimental determination present the same shape and monotonically decrease with empirical methods T_1 and T_2. the distinction at C_{11} consist in the fact that at lower temperatures (T < 523 K) a slight deviation appears between theory and experiment which disappears with increasing temperature. For C_{44} a slight deviation appears between experiment and method T_2 towards higher temperatures (T > 523 K). Regarding C_{12}, the experimental and method T_1 are in the same good approximation. With the exception at some slight deviations we can say that there is an identity between the three methods found, which prove the

validity of the empirical methods T_1 and T_2 and the exactness of the values of the thermal coefficients of elastic constants.

4. Discussion

4.1. Nonlinearity parameter, thermoelastic modulus and bulk modulus
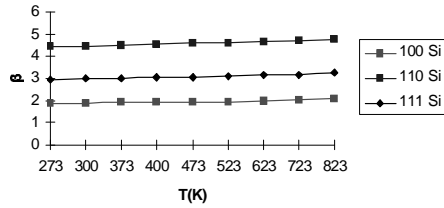
Fig. 3. Dependence of the nonlinearity parameter β on the temperature for the three crystallographic.
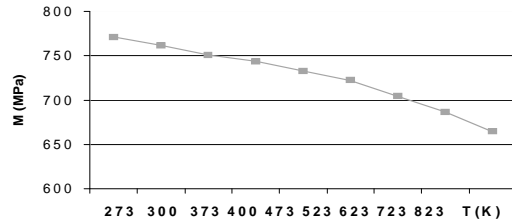
Fig. 4. The semilogaritmic plot of temperature dependence of the termoelastic modulus M.

Fig. 3 shows the dependence of the nonlinearity parameter β on the temperature for the three-crystallographic axis for n-Si. For the n-Si sample the plots show that the highest values are obtained for the [110] axis. Temperature variations are insignificant after the presented orientation, thus after [100] it is just 9.2%, after [111] is 8.5% and after [110] is just 6.8%.
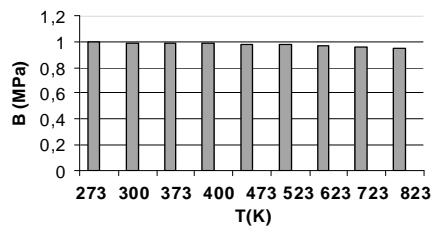
Fig. 5. Temperature plots of the bulk modulus.

For n-Si the semilogaritmic plot of temperature dependence of the thermoelastic modulus M is shown in Fig. 4. The small deviations between the extreme temperatures for Si (0.2%) show that this parameter is invariant to temperature variation. Fig. 5 shows the dependence of the compressional modulus bulk B on the temperature; this parameter appears constant for n-Si.

Table 2. Values for the nonlinearity parameter K_2, K_3 and β by the three axes at 300 K.

	[100]	[110]	[111]
K_2	1.69	1.96	2.05
K_3	-8.25	-14.74	-1237
β	1.88	4.47	3.03

5. Conclusions

The values of the nonlinearity parameter β, K_2 and K_3 by the three axes at 300 K for Si are presented in Table 2 and can be compared with the values reported in [9]. For the temperature

variation of the nonlinearity parameter, we consider that the elastic constants of the 3rd order are temperature independent. The same is valid for K_3 values in [9].

Regarding elastic constants C_{ij} we can conclude as it follows:

- the empirical relations found by the two methods (T_1 and T_2) present similarly graphics to those obtained by experimental determination;
- there is a small variation at C_{11} and C_{44} in the graphics according to the method T_2 around T = 523 K while maintaining it almost constant in the rest of temperature range;
- the compression bulk modulus appears constant for n-Si;
- we have determined the thermal coefficients of elastic constants for n-Si;
- we have found empirical relations by the two methods of C_{ij} variation for n-Si in the considered temperature range and we consider that by this assumption which have been made we can extend the whole range of temperature;
- the temperature variations for the nonlinearity parameter are insignificant by the axes (9.2% [100], 8.5%[111]);
- we have calculated the elastic anisotropy factor and we observed that this factor is a constant in the temperature range and is equal to 1.54±0.06 being in good agreement with those found in literature [14], [15];
- we considered that the anisotropy factor is independent of the temperature for the n-Si and for all elements of the cubic system.

The differences, which appear in the values of the parameter found by us and those from literature are due to the following causes:

- the conversion from the propagation velocity in elastic constants [11];
- multiple reflections occuring as a result of the increase of the ultrasound beam path because of the use of a buffer-rod;
- the influence of the nonparallelism of the lateral surfaces of the buffer-rod and of the samples.

References

[1] Kyung-Young Ihang, Kyung-Cho Kim: Ultrasonics **37**, 39 (1999).
[2] R. F. S Hearmon: Solid State Communications **37**, 915 (1981).
[3] R. Truell, C. Elbaum, B. Chick: Ultrasonic methods in Solid State Physics, Academic Press 14, 1968.
[4] J. and H. KrautKramer: Ultrasonic testing of materials, Spinger Verlag, 23 (1977)
[5] G. Leibfried W. Ludwig: Solid State Physics **12**, 45 (1961).
[6] G. Simon: Journal of Physics Chemistry Solids **28**, 35 (1967).
[7] D. C. Hurley, D. Balzar, P. T. Purtscher, W.Hollman: Journal of Applied Physics **83**, 4584 (1998)
[8] J. Philip, M. A. Breazeale: Ultrasonics Symposium, 1006 (1980).
[9] W. P. Mason: Physical Acoustics, Academic Press **III**, B 261 (1965).
[10] D. T. Queheillalt, H. N. G. Wadley: Journal of Applied Physics **83**, 4124 (1998).
[11] P. Petculescu: Insight-British Journal of Nondestructive Testing **12**, 880 (1996).
[12] W. Ledbetter: Ultrasonics **1**, 10 (1985).
[13] P. Petculescu: Studii si Cercetari de Fizica **4**, 831 (1980).
[14] Yu. A. Burenkov, S. P. Nikanorov, A. V. Stepanov: Sov Physics-Solid State **12**, 1940 (1973).
[15] Yu. A. Burenkov, S. P. Nikanorov: Sov Physics-Solid State **16**, 963 (1974).
[16] H. J. McSkimin, P. Andreatch: Journal of Applied Physics **35**, 2161 (1964).
[17] J. J. Hall: Physical Reviw **161**, 765 (1967).
[18] M. Ezz-El-Arab: Physical Review **161**, 317 (1972).
[19] I. Sirotin, M. P. Saskolskaia: Fizica Cristalelor (Crystal Physics) (roum.) Bucharest, 386 (1981).